

Contents lists available at [SciVerse ScienceDirect](http://SciVerse.ScienceDirect.com)

## Physics Letters B

[www.elsevier.com/locate/physletb](http://www.elsevier.com/locate/physletb)

## Polarization of a stored beam by spin-filtering

W. Augustyniak<sup>a</sup>, L. Barion<sup>b</sup>, S. Barsov<sup>c</sup>, U. Bechstedt<sup>d,e</sup>, P. Benati<sup>b</sup>, S. Bertelli<sup>b</sup>, V. Carassiti<sup>b</sup>, D. Chiladze<sup>f</sup>, G. Ciullo<sup>b</sup>, M. Contalbrigo<sup>b</sup>, P.F. Dalpiaz<sup>b</sup>, S. Dymov<sup>g,h</sup>, R. Engels<sup>d,e</sup>, W. Erwen<sup>e,i</sup>, M. Fiorini<sup>b</sup>, M. Gaisser<sup>d,e</sup>, R. Gebel<sup>d,e</sup>, P. Goslaswski<sup>j</sup>, K. Grigoriev<sup>c,d,e</sup>, G. Guidoboni<sup>b</sup>, A. Kacharava<sup>d,e</sup>, A. Khoukaz<sup>j</sup>, A. Kulikov<sup>h</sup>, H. Kleines<sup>i,e</sup>, G. Langenberg<sup>d,e</sup>, A. Lehrach<sup>d,e</sup>, P. Lenisa<sup>b,\*</sup>, N. Lomidze<sup>f</sup>, B. Lorentz<sup>d,e</sup>, G. Macharashvili<sup>h,d,f</sup>, R. Maier<sup>d,e</sup>, B. Marianski<sup>a</sup>, S. Martin<sup>d,e</sup>, D. Mchedlishvili<sup>f</sup>, S. Merzliakov<sup>h,d,e</sup>, I.N. Meshkov<sup>h</sup>, H.O. Meyer<sup>k</sup>, M. Mielke<sup>j</sup>, M. Mikirtychiants<sup>c,d,e</sup>, S. Mikirtychiants<sup>c,d,e</sup>, A. Nass<sup>d,e</sup>, M. Nekipelov<sup>d,e</sup>, N. Nikolaev<sup>d,e,l</sup>, M. Nioradze<sup>f</sup>, D. Oellers<sup>b,d,e</sup>, M. Papenbrock<sup>j</sup>, L. Pappalardo<sup>b</sup>, A. Pesce<sup>b</sup>, A. Polyanskiy<sup>d,e,m</sup>, D. Prasuhn<sup>d,e</sup>, F. Rathmann<sup>d,e</sup>, J. Sarkadi<sup>d,e</sup>, A. Smirnov<sup>h</sup>, H. Seyfarth<sup>d,e</sup>, V. Shmakova<sup>h,d</sup>, M. Statera<sup>b</sup>, E. Steffens<sup>g</sup>, H.J. Stein<sup>d,e</sup>, H. Stockhorst<sup>d,e</sup>, H. Straatman<sup>n,e</sup>, H. Ströher<sup>d,e</sup>, M. Tabidze<sup>f</sup>, G. Tagliante<sup>o</sup>, P. Thörnngren-Engblom<sup>b,p</sup>, S. Trusov<sup>r,q</sup>, A. Trzcinski<sup>a</sup>, Yu. Valdau<sup>d,e,c</sup>, A. Vasiliev<sup>c</sup>, K.M. von Würtemberg<sup>s</sup>, Chr. Weidemann<sup>b,d,e</sup>, P. Wüstner<sup>i,e</sup>, P. Zupranski<sup>a</sup>

<sup>a</sup> National Centre for Nuclear Research, 00681 Warsaw, Poland<sup>b</sup> Università di Ferrara and INFN, 44122 Ferrara, Italy<sup>c</sup> St. Petersburg Nuclear Physics Institute, 188350 Gatchina, Russia<sup>d</sup> Institut für Kernphysik, Forschungszentrum Jülich GmbH, 52425 Jülich, Germany<sup>e</sup> Jülich Center for Hadron Physics, 52425 Jülich, Germany<sup>f</sup> High Energy Physics Institute, Tbilisi State University, 0186 Tbilisi, Georgia<sup>g</sup> Physikalische Institute II, Universität Erlangen-Nürnberg, 91058 Erlangen, Germany<sup>h</sup> Laboratory of Nuclear Problems, Joint Institute for Nuclear Research, 141980 Dubna, Russia<sup>i</sup> Zentralinstitut für Elektronik, Forschungszentrum Jülich GmbH, 52425 Jülich, Germany<sup>j</sup> Institut für Kernphysik, Universität Münster, 48149 Münster, Germany<sup>k</sup> Physics Department, Indiana University, Bloomington, IN 47405, USA<sup>l</sup> L.D. Landau Institute for Theoretical Physics, 142432 Chernogolovka, Russia<sup>m</sup> Institute for Theoretical and Experimental Physics, 117218 Moscow, Russia<sup>n</sup> Zentralabteilung Technologie, Forschungszentrum Jülich GmbH, 52425 Jülich, Germany<sup>o</sup> INFN, Sezione di Bari, 70126 Bari, Italy<sup>p</sup> Department of Physics, Royal Institute of Technology, SE-10691, Stockholm, Sweden<sup>q</sup> Skobeltsyn Institute of Nuclear Physics, Lomonosov Moscow State University, 119991 Moscow, Russia<sup>r</sup> Institut für Kern- und Hadronenphysik, Forschungszentrum Rossendorf, 01314 Dresden, Germany<sup>s</sup> Department of Physics, Stockholm University, SE-10691, Stockholm, Sweden

## ARTICLE INFO

## Article history:

Received 23 September 2012

Received in revised form 10 October 2012

Accepted 10 October 2012

Available online 15 October 2012

Editor: D.F. Geesaman

## Keywords:

Polarized beams

Storage rings

Antiprotons

## ABSTRACT

The PAX Collaboration has successfully performed a spin-filtering experiment with protons at the COSY-ring. The measurement allowed the determination of the spin-dependent polarizing cross section, that compares well with the theoretical prediction from the nucleon–nucleon potential. The test confirms that spin-filtering can be adopted as a method to polarize a stored beam and that the present interpretation of the mechanism in terms of the proton–proton interaction is correct. The outcome of the experiment is of utmost importance in view of the possible application of the method to polarize a beam of stored antiprotons.

© 2012 Elsevier B.V. Open access under [CC BY license](http://creativecommons.org/licenses/by/3.0/).

## 1. Introduction

Although a number of methods to provide polarized antiproton beams have been proposed more than 20 years ago [1] and

\* Corresponding author.

E-mail address: [lenisa@fe.infn.it](mailto:lenisa@fe.infn.it) (P. Lenisa).

recently reviewed [2], no polarized antiproton beams have been produced so far, with the exception of a low-intensity and low-quality, secondary beam from the decay of anti-hyperons that has been realized at Fermilab [3].

An intense beam of polarized antiprotons will open new experimental opportunities to investigate the still unknown structure of the nucleon. We remind, for instance, the first direct measurement of the transversity distribution of the valence quarks in the proton, a test of the predicted opposite sign of the Sivers-function, related to the quark distribution inside a transversely polarized nucleon in Drell–Yan as compared to semi-inclusive deep-inelastic scattering, and a first measurement of the moduli and the relative phase of the time-like electric and magnetic form factors  $G_{E,M}$  of the proton [4].

In principle, an initially unpolarized beam in a storage ring can be polarized by two methods. In the case of a beam of spin- $\frac{1}{2}$  particles (with two spin states) this might be achieved by either selectively reversing the spin of particles in one spin state (“flipping”) or by selectively discarding particles in one spin state (“filtering”).

Spin-flipping would be preferable over spin-filtering as it would offer the advantage of polarizing the beam not affecting its intensity. Unfortunately, no viable method exploiting spin-flipping has been proposed so far. In a previous work [5], the PAX Collaboration presented a measurement invalidating a proposal to use the flipping method to polarize a stored antiproton beam by means of the interaction with a co-moving polarized positron beam.

Prior to the work presented here, only one experiment had shown that the in-situ polarization build-up of a stored hadron beam actually works. This experiment was performed by the FIL-TEX group at the TSR ring in Heidelberg in 1992 [6] and exploited spin-filtering on a 23 MeV stored proton beam, in the presence of a polarized atomic hydrogen target.

The motivation for the experiment presented in this Letter was to provide an additional measurement to the existing one, confirming the validity of the filtering-method to polarize a stored beam, and to test the present theoretical understanding of the mechanism [7–9] under different experimental conditions.

## 2. Principle of the measurement

The measurement performed at the COSY storage-ring (Forschungszentrum-Jülich) allowed the extraction of the spin-dependent part of the proton–proton cross section when both particles are transversely polarized. The task was accomplished by measuring the polarization buildup induced in a stored beam through the interaction with a polarized hydrogen target. Since the total cross section is different for parallel and antiparallel orientations of the spins of beam and target protons, one spin orientation of the beam particles is depleted at a higher rate than the other one and the circulating beam becomes increasingly polarized, while the intensity decreases with time. In the following, we assume the target polarization to be vertical. The beam is considered to initially consist of equal fractions of particles with spin up and spin down. The total interaction cross section for the beam with the target can be expressed as [10]

$$\sigma_t = \sigma_0 \pm Q \sigma_1 \quad (1)$$

where  $Q$  is the target polarization,  $\sigma_0$  denotes the spin-independent part, and  $\sigma_1$  the spin-dependent part of the total cross section. The positive and negative signs apply to the fraction of the beam particles whose spin is parallel ( $\uparrow\uparrow$ ) or antiparallel ( $\uparrow\downarrow$ ) to the spin of the target, respectively.

As a consequence of the interaction, the intensity of the spin-up and spin-down protons in the ring decreases exponentially with

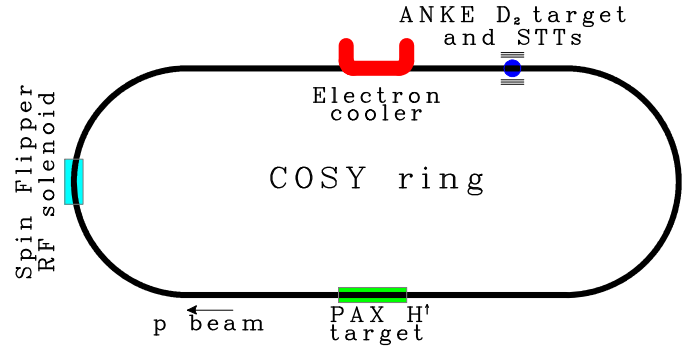


**Fig. 1.** Schematic view of the COSY storage ring. The polarized hydrogen target is installed in one of the straight sections of the ring; the RF solenoid of the Spin Flipper is located in one of the arcs, its use is explained in more detail in the text; the Electron Cooler, followed by the detector setup with Silicon Tracking Telescopes (STTs) to determine the beam polarization, is installed in the second straight section.

different time constants leading to a polarization buildup as function of time

$$P(t) = \frac{N^\uparrow(t) - N^\downarrow(t)}{N^\uparrow(t) + N^\downarrow(t)} = \tanh\left(\frac{t}{\tau_1}\right). \quad (2)$$

The spin-dependent effective polarization buildup cross section  $\tilde{\sigma}_1$  can be extracted from the observed time constant  $\tau_1$  of the buildup rate via

$$\frac{dP}{dt} \approx \frac{1}{\tau_1} = \tilde{\sigma}_1 Q d_t f \quad (3)$$

where  $d_t$  is the target areal density in atoms/cm<sup>2</sup>,  $f$  the particle revolution frequency and  $\tilde{\sigma}_1$  indicates the effective polarizing cross section which accounts for the fact that only protons scattered at angles larger than the acceptance angle of the storage ring  $\theta_{acc}$  contribute to the spin-filtering process  $\tilde{\sigma}_1 = \sigma_1 (\theta > \theta_{acc})$ . We will refer to this effect in Section 6, where we will give a theoretical estimate for  $\tilde{\sigma}_1$  (see Eq. (13)).

## 3. Experimental apparatus

An overview of the COSY machine with the installations utilized in the investigation is shown in Fig. 1. The two main components of the experimental apparatus used for the measurement are the polarized hydrogen gas target, installed at the PAX interaction point, and the beam polarimeter consisting of a deuterium-cluster target of the ANKE experiment surrounded by a system of Silicon Tracking Telescopes (STTs). Phase space cooling of the stored beam is achieved by the Electron Cooler, and the vertical polarization of the stored beam can be reversed using the Spin Flipper solenoid.

### 3.1. Polarized target

The PAX polarized target, shown in Fig. 2, consists of a polarized Atomic Beam Source (ABS), a storage cell, and a diagnostic system. The ABS [11] injects polarized hydrogen atoms into the cell, a sample of the gas diffuses from the center of the cell through a side tube into the diagnostic system. This consists of a Breit–Rabi polarimeter (BRP) [12] measuring the atomic polarization and a Target–Gas Analyzer (TGA) [13] determining the relative fraction of atoms and molecules. A set of coils mounted on the scattering chamber provided the weak vertical holding field ( $\approx 10$  G) requested to orient the target polarization

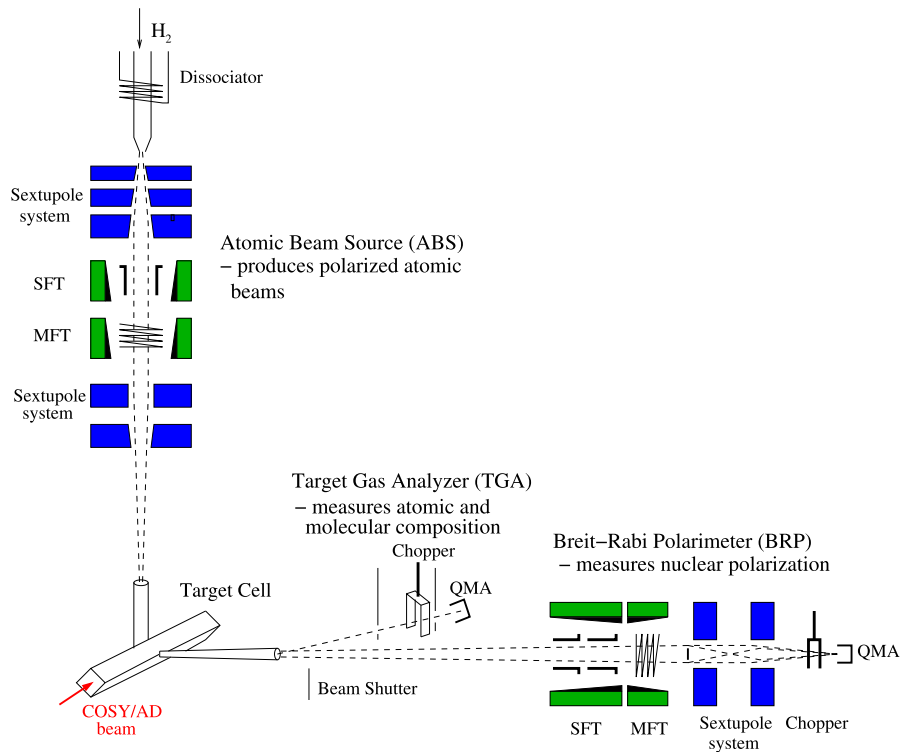


**Fig. 2.** Schematic drawing of the PAX polarized target with the ABS in the vertical position, the storage cell on the ring axis, and the target diagnostic system in the horizontal position. The Target Gas Analyzer (TGA) determines the atomic to molecular fraction of the effusive beam from the storage cell, while the Breit-Rabi Polarimeter (BRP) measures the degree of polarization of the atomic sample.

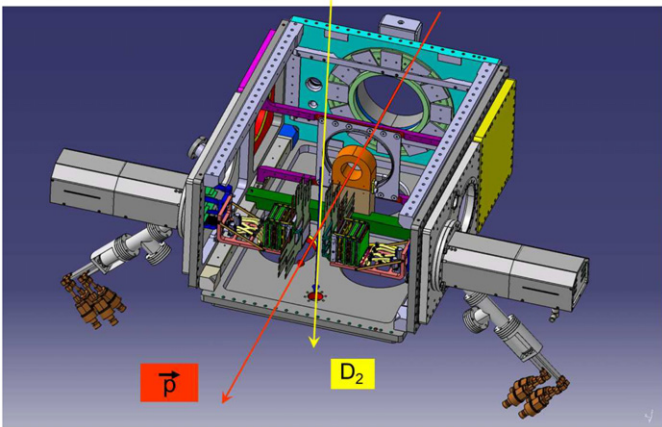


**Fig. 3.** Experimental setup for the measurement of the beam polarization. The cluster target beam comes from the top and traverses the beam stored in the machine. Recoil deuterons are detected by two Silicon Tracking Telescopes (STTs) left and right to the beam.

### 3.2. Beam polarimeter

The beam polarization has been measured by detecting elastically scattered protons and deuterons off the ANKE cluster target (see Section 5.1 for a description of the method). Two Silicon Tracking Telescopes (STT) [14] have been placed left and right the deuterium cluster target [15], with respect to the proton beam, at the ANKE interaction point (see Fig. 3). The ANKE deuterium cluster target provides a beam of about 10 mm diameter with an integrated areal density of  $1.5 \cdot 10^{14}$  atoms/cm<sup>2</sup>. Each telescope comprises three position-sensitive detectors, oriented parallel to the beam direction. The first (second) layer is 65  $\mu$ m (300  $\mu$ m)

thick, with an active area of 51 mm by 66 mm. They are located at a distance of 28 mm (48 mm) away from the beam axis. The third layer, consisting of 5 mm thick detectors, is located at a distance of 61 mm from the beam axis. Within the mechanical constraints of the detector support, the telescope position with respect to the interaction region is chosen to optimize the figure-of-merit for the  $pd$  analyzing reaction.

### 4. Spin filtering cycle

In order to perform the measurement, dedicated spin-filtering cycles have been introduced. The sequence of operations in any cycle is as follows:

- An unpolarized proton beam is injected in the COSY ring at a beam energy of 45 MeV. The beam is cooled and subsequently accelerated to 49.3 MeV. This energy has been chosen for the spin-filtering experiments, because of existing data of the analyzing power in proton–deuteron elastic scattering [16]. The typical number of particles injected and accelerated in every cycle was about  $5 \cdot 10^9$ .
- At this point the spin-filtering starts. Polarized hydrogen is injected into the storage cell at the PAX interaction point. The holding field coils are powered on in either up ( $\uparrow$ ) or down ( $\downarrow$ ) orientation for the duration of the spin-filtering period. Two different durations for the spin-filtering periods have been adopted: one lasting for 12 000 s, and a longer one of 16 000 s, corresponding to about 1.5 and 2 times the measured beam-lifetime (8000 s). These spin-filtering times were judiciously chosen to optimize the relative statistical uncertainty of the final result.
- At the end of the spin-filtering period, the PAX polarized target is switched off, the ANKE deuterium-cluster target is switched

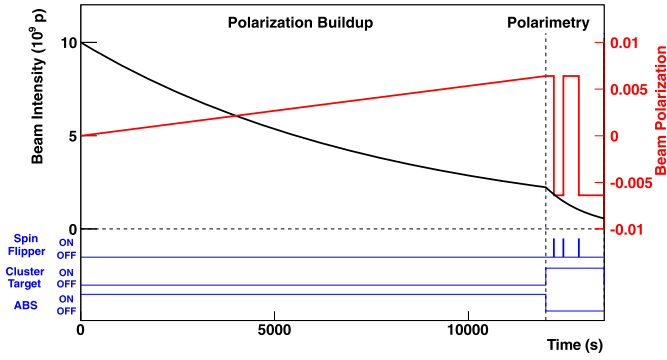


**Fig. 4.** Schematic representation of a spin-filtering cycle. The black curve represents the beam current (left scale), while the red one shows the polarization, induced in the beam (right scale). With the PAX polarized target on, while the beam current decreases, the polarization in the beam builds up. At the end of the spin-filtering cycle, the ANKE cluster target is used and the spin-flipper is switched on three-times to allow for the measurement of the beam polarization. Cycles with different orientations of the target holding field (HF) have been performed. (For interpretation of the references to color in this figure legend, the reader is referred to the web version of this Letter.)

on and the data acquisition of the beam polarimeter starts. During the beam polarization measurement, the beam polarization is reversed three times using the spin-flipper. This allows for the determination of the induced beam polarization within each cycle, thereby reducing systematic errors. The total duration of the polarization measurement in each cycle was 2500 s.

Spin-filtering cycles have been repeated for different directions of the target holding fields: up ( $\uparrow$ ) or down ( $\downarrow$ ). A typical spin-filtering cycle is depicted in Fig. 4.

#### 4.1. Zero measurement

To provide a cross-check for the zero polarization of the detector, a series of dedicate cycles has been carried out in addition. To be as close as possible to the experimental conditions of a standard filtering cycle, the zero measurement cycle reflected exactly the same sequence of operations, differing only in the number of injected particles ( $< 1 \cdot 10^9$ ), equal to the number of particles in the ring after spin-filtering and in the duration of the spin-filtering part (180 s vs 12000 s or 16000 s).

## 5. Data analysis

As described in Section 2, the effective polarizing cross section can be derived from the measurement of the rate of polarization buildup in the stored beam,

$$\tilde{\sigma}_1 = \frac{dP}{dt} \frac{1}{Q d_t f}. \quad (4)$$

In this section we briefly describe how the individual factors appearing in Eq. (4) have been determined.

### 5.1. Polarization buildup

The beam polarization is measured by using  $p^{\uparrow}d$  elastic scattering. The cross section for the interaction of a transversely polarized proton beam impinging on an unpolarized deuterium target is given by

$$\frac{d\sigma}{d\Omega}(\theta, \phi) = \frac{d\sigma_0}{d\Omega} [1 + P A_y(\theta) \cos\phi] \quad (5)$$

where  $\frac{d\sigma_0}{d\Omega}$  is the unpolarized cross section,  $A_y(\theta)$  is the analyzing power,  $\theta$  and  $\phi$  are the polar and the azimuthal scattering angle in the laboratory system, respectively. Precise analyzing power data are available from [16], and differential cross sections have been measured at a nearby energy ( $T_p = 46.3$  MeV) [17].

Deuterons and protons stopped in the second or third detector layer can be clearly identified by means of the  $\Delta E/E$  method. Since the data were taken below the pion-production threshold, an identified deuteron ensures that elastic scattering took place. In order to distinguish elastically scattered protons from the ones that stem from deuteron breakup, a cut based on the relation between deposited energy and scattering angle has been applied. The contamination of the selected elastic proton sample from protons originating from  $pd$ -breakup events is estimated to be less than 3%. The presented analysis is based on a total number of  $8.6 \cdot 10^6$  identified deuterons and  $1.6 \cdot 10^6$  identified protons.

The beam polarization  $P$  is derived from the asymmetry determined using the so-called cross ratio-method [18]. The method provides a cancellation of all first order false asymmetries caused by differences in acceptance, efficiency, and integrated luminosity in the two detectors. The cross ratio  $\delta$  is defined by means of the rates  $Y(\theta, \phi)_{R,L,\uparrow,\downarrow}$  detected in the left (L) and right (R) detectors for data samples with spin up ( $\uparrow$ ) and down ( $\downarrow$ ) beam polarizations,

$$\delta = \sqrt{\frac{Y_{L\uparrow}(\theta, \phi) \cdot Y_{R\downarrow}(\theta, \phi)}{Y_{L\downarrow}(\theta, \phi) \cdot Y_{R\uparrow}(\theta, \phi)}} = \frac{1 + P A_y(\theta)}{1 - P A_y(\theta)}. \quad (6)$$

The asymmetry is defined as

$$\epsilon = \frac{\delta - 1}{\delta + 1} = P A_y(\cos\phi). \quad (7)$$

In Eq. (5), the average of the trigonometric function accounting for the azimuthal dependence of the analyzing power over the detector acceptance in the interval  $-25^\circ < \phi < 25^\circ$  has been approximated to unity without affecting the measured asymmetry. The selected events are sorted in bins of  $3^\circ$  width. The polarization is extracted by scaling the measured asymmetry using a fit based on a 5th order polynomial of the analyzing power taken from [16]. As an example, the extracted asymmetries for deuterons after 12000 s spin-filtering cycle are presented in Fig. 5 (upper panel) as a function of the deuteron scattering angle in the laboratory system. The plot presents the asymmetry of the detected deuterons in the range  $53^\circ < \theta < 74^\circ$ , while it reports the asymmetry of the reconstructed deuterons from the identified protons in the range  $30^\circ < \theta < 51^\circ$ . The line represents the result of the overall fit.

In order to investigate fake asymmetries as possible sources of systematic errors, the same analysis procedure has been applied to the zero measurement, where no spin-filtering took place and no polarization was induced in the beam (Fig. 5, lower panel). This measurement can be interpreted as a determination of the systematic error of the beam polarization.

The beam polarization obtained from spin-filtering cycles of different length for the two target spin-orientations is presented in Fig. 6. The plot presents the total acquired statistics including events where either a deuteron or a proton from elastic scattering were identified. We mention here that although the number of identified protons is about a factor 5 smaller than the number of identified deuterons, the contributions of the two samples to the statistical uncertainty are comparable due to the different magnitude of the corresponding analyzing powers. Note that a change in sign of the target polarization, realized by reversing the holding field, causes a change in sign in the induced beam polarization. In



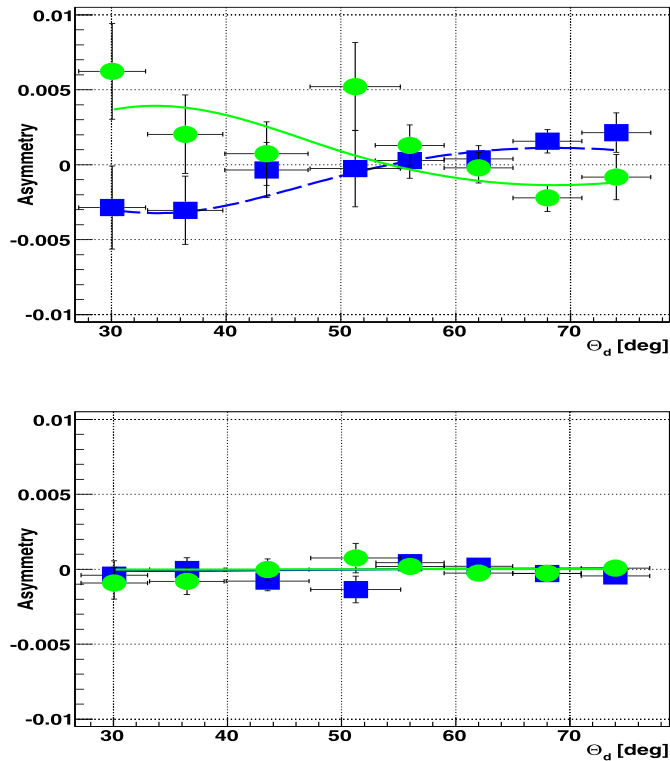


**Fig. 5.** Upper panel: Measured asymmetry from spin-filtering with different orientations of the target polarization for the 12000 s filtering cycle. The asymmetry for the detected deuterons is presented in the range  $53^\circ < \theta < 74^\circ$ , while the asymmetry of the reconstructed deuterons from the identified elastic protons is reported in the range  $30^\circ < \theta < 51^\circ$ . Lower panel: Result of the analysis of runs where no beam polarization was induced by making the filtering time very short (zero measurement). The green circles and blue squares indicate positive and negative orientations of the target holding field and consequently of the target polarization. (For interpretation of the references to color in this figure legend, the reader is referred to the web version of this Letter.)

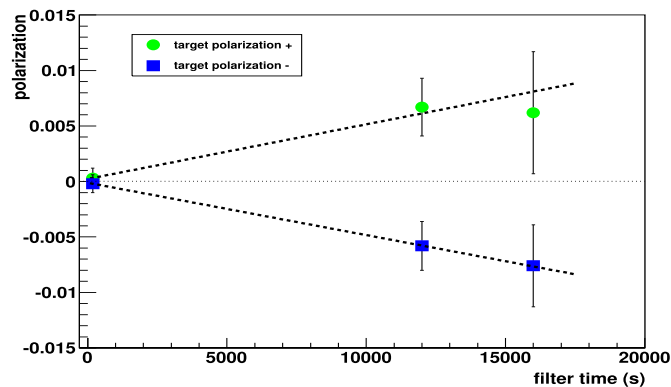


**Fig. 6.** Polarization induced in the beam after filtering for different times and different signs of the target polarization. The induced polarization in the beam has the same sign as the target polarization, reflecting the negative sign of the polarizing cross section.

particular, a positive target polarization induces a positive polarization buildup in the stored beam and vice versa. This is a reflection of the negative value of the polarizing cross-section  $\tilde{\sigma}_1$ .

A linear fit to the five points shown in Fig. 6 allows us to determine  $\frac{dP}{dt} = (4.8 \pm 0.8) \cdot 10^{-7} \text{ s}^{-1}$ .

## 5.2. Target polarization

The polarized target ran smoothly and reliably delivered a stable performance over time. The average target polarization  $Q$  can be expressed through

$$Q = \alpha P_{at}, \quad (8)$$

where  $\alpha$  is the hydrogen atomic fraction, given by

$$\alpha = \frac{n_H}{n_H + 2n_{H_2}} \quad (9)$$

and  $P_{at}$  is the atomic polarization, given by

$$P_{at} = \frac{n_{H\uparrow} - n_{H\downarrow}}{n_{H\uparrow} + n_{H\downarrow}}. \quad (10)$$

After injection into the target cell, the polarized atoms undergo collisions with the walls of the target cell that can cause recombination and depolarization. The magnitude of the average target polarization  $Q$ , as seen by the proton beam passing through the cell is limited between the polarization value of atoms injected into the cell from the atomic beam source (upper bound:  $Q^{inj}$ ), and the value determined by the target polarimeter (lower bound:  $Q^{meas}$ ). Due to the geometry of the storage cell and the sample tube, the measured gas sample undergoes more than 1000 wall collisions before it leaves the sampling tube, while there are only about 300 wall collisions in the cell tube itself.

- *Injected polarization into the cell from the ABS ( $Q^{inj}$ ).*

The value of the atomic fraction of the particles injected into the storage cell from the ABS is  $\alpha^{inj} = 0.93 \pm 0.03$  [11]. By adopting the ABS sextupole transmissions, measured in [11] and an efficiency of 0.98 for the  $m_{23}$  transition adopted to select the hydrogen hyperfine state  $|1\rangle$  used in the measurement, we obtain for the polarization of the atoms injected into the cell a value of  $P_{at}^{inj} = 0.85 \pm 0.01$ . Combining the two values mentioned above, we obtain the total polarization of the particles injected into the cell  $Q^{inj} = \alpha^{inj} P_{at}^{inj} = 0.79 \pm 0.03$ . We note here that the hydrogen molecule formed by recombination on the storage cell walls of polarized atoms, can retain the nuclear polarization and this can in principle affect the target polarization [19,20]. Actually, under the weak holding field conditions of the present experiment, the molecular polarization can be assumed to be negligible (see Fig. 2 of Ref. [19]).

- *Measured target polarization ( $Q^{meas}$ ).*

The atomic fraction was continuously monitored by the Target Gas Analyzer (TGA) during the measurement, and the observed values were stable within  $\pm 0.01$  with a central value  $\alpha^{TGA} = 0.85 \pm 0.01$ . The atomic polarization was continuously monitored during the measurement as well, and the observed value was stable within  $\pm 0.01$  with a central value of  $P_{at}^{BRP} = 0.79 \pm 0.01$ . Combining the two above-mentioned values, we obtain the measured total target polarization of  $Q^{meas} = \alpha^{TGA} P_{at}^{BRP} = 0.671 \pm 0.014$ .

- *Estimation of the average polarization in the cell.*

Without making any assumption about the status of the cell surface, the average target polarization as seen by the stored beam passing through the storage cell  $Q$  can be assumed to be between the injected and measured values  $0.67 = Q^{meas} < Q < Q^{inj} = 0.79$ . By assuming the most probable, uniform distribution in this interval, we obtain  $Q = 0.73 \pm 0.05$ .

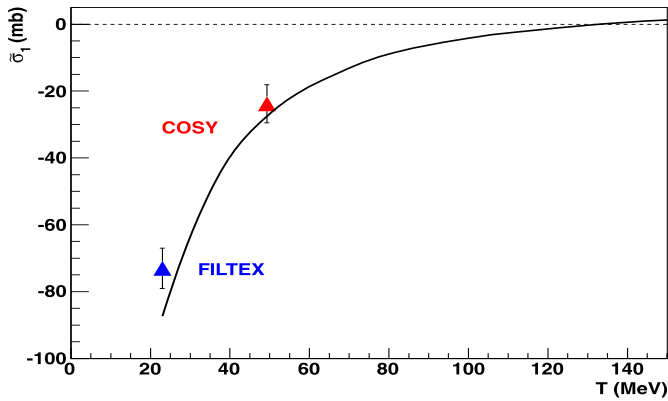


**Fig. 7.** Measured spin-dependent polarizing cross section for the interaction (only statistical errors are shown). The solid line represents the prediction from the SAID database. The prediction are basically independent from the ring-acceptance in the interval of values interested by the TSR and COSY rings.

### 5.3. Target thickness

The target thickness has been measured using the beam energy loss method which in turn is deduced from a shift of the orbit frequency of the coasting beam [21],

$$d_t = (5.5 \pm 0.2) \cdot 10^{13} \frac{\text{atoms}}{\text{cm}^2}. \quad (11)$$

## 6. Result and discussion

By substituting the results of the previous Section in Eq. (4), together with the revolution frequency  $f$  of 510 032 Hz in the ring at the experiment energy of  $T_p = 49.3$  MeV, we finally obtain:

$$\bar{\sigma}_1^{\text{meas}} = -23.4_{\pm 1.9}^{\pm 3.9(\text{stat.})} \text{ mb}. \quad (12)$$

The measured cross section can be compared to the predicted one, based on the present knowledge of the  $pp$  spin-dependent interaction as given in the SAID data base. In particular, the theoretical value of the effective polarizing cross section  $\bar{\sigma}_1^{\text{theor}}$  can be obtained by [5]:

$$\bar{\sigma}_1^{\text{theor}} = 2\pi \int_{\theta_{\text{acc}}}^{\pi/2} \frac{1}{2} (A_{00nn} + A_{00ss}) \frac{d\sigma_0}{d\Omega} \sin \theta d\theta = -26.9 \text{ mb}. \quad (13)$$

The spin-correlation factors in Eq. (13) are taken from the SAID database [22]. The acceptance angle  $\theta_{\text{acc}}$  of the COSY ring has been directly measured by a movable frame system installed at the PAX interaction point prior to the spin-filtering measurements. The measured acceptance angle at the position of the target amounts to:  $\theta_{\text{acc}} = 6.15 \pm 0.17$  mrad [23].

The spin-dependent cross-section measured at COSY is presented in Fig. 7 together with the other existing measurement performed by the FILTEX collaboration [6]. The solid line represents the theoretical prediction from the SAID data base. The good agreement between measurement and theory confirms that spin-filtering of a stored proton beam is well-described taking into account the contributions from proton–proton scattering [7–9].

It should be noted that the polarization buildup rates in the TSR experiment were about a factor seven larger than in the present COSY experiment ( $3.6 \cdot 10^{-6} \text{ s}^{-1}$  vs  $4.8 \cdot 10^{-7} \text{ s}^{-1}$ ). On the one hand, the polarizing cross section in the spin-filtering experiment at COSY is about a factor three smaller (see Fig. 7), on the other, COSY is about three times larger in circumference than the TSR,

hence the smaller revolution frequency  $f$  reduces further the rate of polarization buildup (see Eq. (3)). The different acceptances of the TSR and COSY rings (4.4 mrad vs 6.1 mrad) do not appreciably influence the polarizing cross section.

## 7. Conclusions

The PAX Collaboration has successfully completed a spin-filtering experiment using a beam of protons at COSY. The measurement has allowed the extraction of the polarizing cross-section in proton–proton interactions and represents a milestone in the field. It confirms that spin-filtering can be effectively used to polarize a stored beam in situ and that our understanding of the mechanism in terms of the proton–proton interaction is correct: the predictions are in excellent agreement with the available data. The achievement is of fundamental importance in view of the possible application of the method to polarize a beam of stored antiprotons. In this respect, the existing theoretical predictions for the polarization buildup with antiprotons are affected by the lack of knowledge of the proton–antiproton interactions and differ by more than a factor 2 [8,24]. For this reason, a direct measurement of the polarizing cross sections in proton–antiproton interactions constitutes an inevitable step towards the design of dedicated polarizer ring [25].

## Acknowledgements

The present work is supported by the EU grants of the Joint Research Activity-I3HP2 (Grant Agreement 227431) and of the ERC Advanced Grant POLPBAR (Grant Agreement 246980).

## References

- [1] A.D. Krisch, A.M.T. Lin, O. Chamberlain (Eds.), Proceeding of the Workshop on Polarized Antiprotons, Bodega Bay, CA, 1985, AIP Conf. Proc., vol. 145, 1986.
- [2] D.P. Barber, N. Buttmore, S. Chattopadhyay, G. Court, E. Steffens (Eds.), Proceedings of the International Workshop on Polarized Antiproton Beams, AIP Conf. Proc., 2008.
- [3] D.P. Grosnick, et al., Nucl. Instr. Meth. A 290 (1990) 269.
- [4] PAX Collaboration, Technical proposal for antiproton–proton scattering experiments with polarization, <http://arxiv.org/abs/hep-ex/0505054>, an update can be found at the PAX website <http://www.fz-juelich.de/ikp/pax>.
- [5] D. Oellers, et al., Phys. Lett. B 674 (2009) 269.
- [6] F. Rathmann, et al., Phys. Rev. Lett. 71 (1993) 1379.
- [7] A. Milstein, V. Strakhovenko, Phys. Rev. E 72 (2005) 066503.
- [8] N. Nikolaev, F. Pavlov, in: Proceedings of the 17th International Spin Physics Symposium (SPIN2006), Kyoto, 2006, arXiv:hep-ph/0601184.
- [9] N.H. Buttmore, D. O'Brien, Eur. Phys. J. A 35 (2008) 47.
- [10] J. Bystricky, F. Lehar, P. Winternitz, J. Phys. 39 (1978) 1.
- [11] A. Nass, et al., Nucl. Instr. Meth. A 505 (2003) 633.
- [12] C. Baumgarten, et al., Nucl. Instr. and Meth. A 482 (2002) 606.
- [13] C. Baumgarten, et al., Nucl. Instr. and Meth. A 508 (2003) 268.
- [14] R. Schleichert, et al., IEEE Trans. Nucl. Sci. 50 (2003) 301.
- [15] A. Khoukaz, et al., Eur. Phys. J. D 5 (1999) 275.
- [16] N.S.P. King, et al., Phys. Lett. B 69 (1977) 2.
- [17] S.N. Bunker, et al., Nucl. Phys. A 113 (1968) 461.
- [18] G. Ohlsen, P. Keaton, Nucl. Instr. Meth. 109 (1973) 41.
- [19] T. Wise, et al., Phys. Rev. Lett. 87 (2001) 042741.
- [20] A. Airapetian, et al., Eur. Phys. J. D 29 (2004) 21.
- [21] H.J. Stein, et al., Phys. Rev. ST-AB 11 (2008) 052801.
- [22] SAID, Nucleon–nucleon scattering database, Center for Nuclear Studies, Department of Physics, George Washington University, USA.
- [23] Chr. Weidemann, PhD thesis, Cologne University, <http://www2.fz-juelich.de/ikp/pax/portal/documents/theses/files/thesisCh.Weidemann.pdf>; PAX-Collaboration, Machine development for spin-filterin studies at COSY, in preparation.
- [24] V.F. Dimitriev, A.I. Milstein, S.G. Salnikov, Phys. Lett. B 690 (2010) 427.
- [25] To this purpose, the PAX Collaboration has submitted a proposal to the CERN-SPSC to measure the spin-dependence of the proton–antiproton interaction at the AD-ring (CERN-SPSC-2009-012; SPSC-P-337).